



Contents lists available at ScienceDirect

Journal of Rock Mechanics and Geotechnical Engineering

journal homepage: www.rockgeotech.org

Full Length Article

Pullout of soil nail with circular discs: A three-dimensional finite element analysis



Saurabh Rawat, Ashok Kumar Gupta*, Anil Kumar

Department of Civil Engineering, Jaypee University of Information Technology, Waknaghat, Solan, 173234, Himachal Pradesh, India

ARTICLE INFO

Article history:

Received 19 February 2017

Received in revised form

4 April 2017

Accepted 7 May 2017

Available online 11 September 2017

Keywords:

Pullout behaviour

Finite element analysis

Soil nail

Circular discs

Dimensionless factors

ABSTRACT

An internal failure mode for a soil-nailed system consists of failure at nail heads, slope facing, nail strength, along grout–soil interface and pullout failure. A better understanding of pullout of soil nail thus becomes important to assess the stability of a soil-nailed system. In the present study, an investigation into the pullout behaviour of soil nail with circular discs along the shaft has been carried out by a three-dimensional finite element analysis using Abaqus/Explicit routine. A total of 67 simulations have been performed to accurately predict the pullout behaviour of soil nail. The soil nail under study has circular discs along its shaft varying in numbers from 1 to 4. The pullout of this soil nail in a pullout test box has been simulated with a constant overburden pressure of 20 kPa acting on the nail. The pullout load–displacement characteristics, stresses around soil nail and failure mechanism during pullout are studied. Variations of dimensionless factors such as normalised pullout load factor and bearing capacity factor have been obtained with different combinations of parameters in terms of relative disc spacing ratio, anchorage length ratio, embedment ratio, diameter ratio and displacement ratio. From the results of analyses, it is found that nail with more circular discs requires higher pullout load. There are critical relative disc spacing ratio and diameter ratio which significantly affect the pullout behaviour of nail.

© 2017 Institute of Rock and Soil Mechanics, Chinese Academy of Sciences. Production and hosting by Elsevier B.V. This is an open access article under the CC BY-NC-ND license (<http://creativecommons.org/licenses/by-nc-nd/4.0/>).

1. Introduction

The overall shear strength of an existing slope or a future slope/cut can be increased by installing closely spaced inclusions termed as 'soil nails'. These soil nails intersect the failure surface of slope and provide reinforcement to the soil-nailed system. Since the soil is weak in tension, tensile strength of these nails is mobilised during slope failure. The internal stability of a soil-nailed system can be assessed by a simple two-zone model (Schlosser, 1982). The potential failure surface divides soil mass into two zones, i.e. active and passive. The soil nail acts as a tie which fastens the active to the passive zone. The front active zone has a tendency to detach itself from the remaining soil mass and cause pullout of soil nails. Thus, a soil nail is subjected to tensile forces during slope failure. Stresses are also mobilised during shearing at the intersection of slip surface with soil nails (Juran, 1985; Bridle and Davies, 1997). However, Geoguide 7 (GEO, 2008) put emphasis on external and internal

failure modes of a soil-nailed system. The internal failure modes are related to failure surface within the soil-nailed ground. Along with failure at nail heads, slope facing, nail strength, and along grout–soil interface, pullout failure is also primarily an internal failure mode. When the nail length in the passive zone is insufficient, it renders a poor pullout resistance per unit length of soil nail. This leads to an occurrence of failure at the grout–soil interface.

Many researchers have carried out experimental as well as analytical studies to comprehend the pullout behaviour of soil nails (Heymann et al., 1992; Milligan and Tei, 1998; Luo et al., 2000; Pradhan et al., 2006; Yin and Su, 2006). Past studies also reflect on the fact that pullout of soil nails depends on various factors such as installation method, overburden stress, grouting pressure, roughness of nail surface, soil dilation, degree of saturation and soil-nail bending (Zhou, 2008). From a large-scale field study, Lum (2007) observed that pullout of soil nails causes cracking in the grout column formed during nail installation. This cracking reduces the composite stiffness but increases the axial strain. This increase in axial strain leads to higher pullout capacity of nails. The overburden pressure is found to increase the normal stress around the nail shaft. The increase in normal stress is found to increase the apparent coefficient of friction between nail and soil interface that

* Corresponding author.

E-mail address: ashok.gupta@juit.ac.in (A.K. Gupta).

Peer review under responsibility of Institute of Rock and Soil Mechanics, Chinese Academy of Sciences.

causes an increase in nail pullout resistance. However, Luo et al. (2000) developed an analytical model to theoretically predict that the actual normal stress acting around a soil nail during pullout is higher than the overburden pressure due to soil dilation. As a result, a higher coefficient of friction than the true soil internal friction is mobilised during soil-nail pullout. To understand the effect of surface roughness on pullout capacity of soil nail, Hong et al. (2003) conducted model tests on the pullout of single and double nails in sand. A large number of variations in parameters regarding surface roughness, nail length to diameter ratio, overburden pressure and group efficiency were also observed. It was concluded that the apparent coefficient of friction at soil-nail interface varies with change in the surface roughness of nail.

Numerical modelling of soil nail pullout has also captured the interest of past researchers (Kao, 2004; Akiş, 2009; Zhou et al., 2009) to further enhance or validate pullout testing. The effect of overburden and soil dilation on pullout capacity of soil nail is modelled using a three-dimensional (3D) finite element analysis by Su et al. (2010) with a conclusion that pullout resistance of soil nail is dependent on constrained dilatancy of soil-nail interface to surrounding soil rather than overburden stress. The accuracy of simulated soil nail pullout by finite element modelling was also validated by Zhou et al. (2011). With the advancement in soil nailing technique, researchers like Tokhi et al. (2016) developed a screw-type soil nail to overcome the installation complexities of soil disturbance and produced spoils identified with conventional grout soil nails. It was observed from experimental and numerical analyses of screw nail that it holds the advantage of easy installation by providing torque with better pullout resistance as compared to conventional soil nails.

The soil nails mounted with parallel circular discs can be driven into ground by pushing and rotation technique. To initiate the horizontal penetration of nail into ground, this type of nail needs to be pushed into ground which splits the soil and displaces it to the sides by a distance equal to the radius of the shaft. This initial soil displacement allows the circular discs to be positioned into soil with small penetration. As the nail is pushed further accompanied by torque at its head, the soil is cut and displaced to the sides. The volume of soil displaced is equal to the volume of circular discs which is similar to a helical plate with small pitch (Perko, 2000). The average distance required to displace the soil for circular disc insertion is approximately equal to half the thickness of the disc (Perko, 2000). Since the thickness of discs in the present study is small, it can easily cut through loose soil and the minimal soil displacements can also be expected. Consequently, soil-nail contact can be reestablished in relatively less time. As the first disc cuts and displaces the soil, it paves way for the following discs to be located at desired locations. Moreover, these soil nails with circular discs can also be used by burying them in advance during reinstating a failed slope or a loose fill slope.

HKIE (2003) reported that to reinstate a failed loose fill slope, the top 3 m of the slope should be excavated and recompacted so as to increase its stability. In such cases, soil nails with circular discs can be placed at desired levels during reconstruction of such slopes after excavation, which will not only reduce compaction efforts but also increase the stability of loose fill slope with much better efficiency than compaction. Some other real application examples of these soil nails can be in cases of newly built embankments, where these nails can be installed easily and effectively owing to weak soil conditions as staged construction of embankment progresses.

Moreover, some researchers have analytically studied helical micropiles (Papadopoulou et al., 2014), multi-plate helical anchors (Merifield, 2011) and helical soil nails (Rawat and Gupta, 2017) by considering helix as circular or conical shape, but have mainly adopted axisymmetric condition, considering that uniform stress–strains are developed during soil nail pullout behaviour. With this constraint of available literature on soil nail with circular discs in 3D finite element

analyses condition, the introduction focused on such soil nails which can be approximated with the nail in the present study.

Based on the literature review, the present work focuses on understanding the pullout behaviour of a soil nail with circular discs along the nail shaft. The 3D finite element analysis of this soil nail is carried out by numerical modelling in Abaqus/Explicit v6.13. Variations in peak pullout capacity (P) with soil nail displacement (u), number of circular discs along the nail shaft ($N = 0, 1, 2, 3$ and 4) and diameter of circular discs (D_c) have been investigated. The optimisation of pullout response is done by considering relative disc spacing ratio ($s/D_c = 1, 1.5, 2, 2.5, 3, 3.5$ and 4). Variations in relative diameter ratio ($D_c/d_s = 1, 2, 3$ and 4), anchorage length ratio (L/D_c), embedment ratio (H/D) and displacement ratio (u/L) are also incorporated to observe the effect on soil nail pullout capacity. The normalised pullout capacity is determined by using a dimensionless factor (P/P_0) and circular disc contribution to soil nail pullout is studied by a bearing capacity factor (N_q). The results obtained from finite element analysis are validated and found in good agreement with testing and numerical results obtained from literature.

2. Problem definition

A soil nail may be positioned at different angles with horizontal inside the soil mass. In the present analysis, soil nail with circular disc is oriented at 0° with horizontal for all cases under study. The soil nail consists of a circular shaft having diameter (d_s) of 15 mm. The number of circular discs along the shaft varies from 1 to 4, i.e. $N = 1, 2, 3$ and 4 . The circular discs have a diameter (D_c) which is considered on the basis of a relative diameter ratio (D_c/d_s). The D_c/d_s ratios used are 1, 2, 3 and 4, resulting in D_c variation of $d_s, 2d_s, 3d_s$ and $4d_s$. The circular discs are evenly spaced along the nail shaft at a specified spacing (s). Different spacings of circular discs are adopted based on a relative spacing ratio (s/D_c) taken as 1, 1.5, 2, 2.5, 3, 3.5 and 4. The variation of s/D_c has been studied for $N = 2, 3$ and 4. With the change in number of circular discs along soil nail shaft, variation in soil nail shaft length beyond the first disc to nail head (L) is used to define anchorage length ratio as L/D_c . The depth of embedment of soil nail from the top surface of pullout box (H) is 500 mm for all parametric variations. An overburden pressure of 20 kPa adopted from Tokhi et al. (2016) is considered to be acting on the surface of pullout box. The general layout of the problem definition to be analysed is given in Fig. 1.

A conventional soil nail consists of shaft embedded in grout column so that during nail pullout, the apparent friction at grout–soil interface is mobilised. It can be visualised that in conventional soil nail, shaft friction contributes significantly to resisting the pullout force. The shear stresses are generated at soil-nail interface around the perimeter of soil nail shaft throughout its anchorage length. These shear stresses are transferred as tensile forces to soil nail. Hence it can be inferred that grout column diameter and length of soil nail behind the potential slip surface govern the pullout of conventional soil nails. Thus, pullout capacity (P) of soil nail as given in FHWA (2003) can be calculated by

$$P = \pi q D_{DH} L \quad (1)$$

where q is the mobilised shear stress acting along the perimeter of soil-nail interface, and D_{DH} is the diameter of drill hole for grouting.

The shear stress acting along the perimeter is a function of normal stress around the soil nail and the interface friction. Since soil is a weaker material in comparison to nail embedded in grout column, it can be said that during pullout, soil will tend to fail before the grout column. This makes the soil–soil interface friction more critical than soil-grout interface friction. Hence the mobilised interface friction is treated as equal to $\tan\phi$, where ϕ is the angle of internal friction of soil. Thus, Eq. (1) can also take a form of

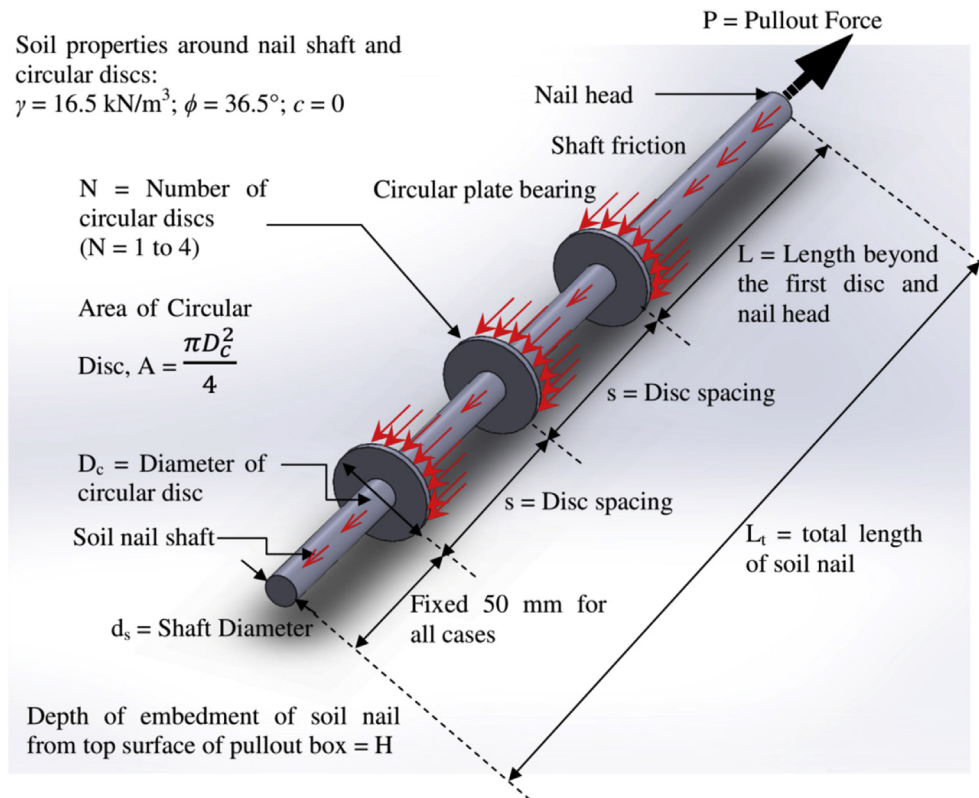


Fig. 1. Problem definition.

$$P = \pi \sigma_v D_{DH} L \tan \phi \quad (2)$$

where σ_v is the normal stress around soil nail determined as the product of unit weight of soil (γ) and height of soil mass above nail.

In the present soil nail, circular disc provides an additional resistance to pullout by increasing the surface area of nail shaft. Due to the addition of circular disc along the nail shaft, an extra bearing is imposed on nail displacement subjected to pullout load. The contribution of circular disc can thus be accounted for by its bearing capacity due to increased area. The pullout of soil nail with circular disc will be a combined action of resistance from the nail shaft and bearing by circular discs. Consequently, Eq. (2) can be modified as

$$P = \pi \sigma_v D_{DH} L \tan \phi + \sum_{i=0}^N (A_i \sigma_v K_0 N_{q_i}) \quad (3)$$

where A_i is the area of circular disc i , K_0 is the coefficient of earth pressure at rest ($K_0 = 1 - \sin \phi$), and N_{q_i} is the bearing capacity factor at disc i .

The simulation of soil nail with circular discs in the present study deals with pullout of soil nail for a condition that soil nail has been left for a sufficient period of time after installation and soil has reestablished full contact with the entire soil nail due to consolidation and creep settlement. The basis for this consideration can be accounted for by the type of soil used for analysis which is dry sand. Sand can be expected to form full contact with nail within a small period of time owing to its zero sensitivity and immediate settlement. Moreover, small thickness of circular discs accounts for negligible disturbances to the surrounding soil, which further simplifies and hastens the soil-nail contact. Due to this in Eq. (3), the pullout resistance is predicted by considering the gross area of disc.

The soil used for pullout simulation is dry sand with zero degree of saturation. Since the soil nail can be installed by burying it in

advance without any grouting and drill hole, the change in soil saturation due to grouting and pore water pressure developed during shearing in sand is also neglected.

It can also be stated that if significant circular disc thickness is considered, the shear resistance provided by the disc side friction will also be added up against soil nail pullout and should be incorporated in Eq. (3). However, in the present analysis, 5 mm thin circular disc is considered with negligible side friction. It can also be concluded theoretically from Eq. (3) that increasing the number of discs will increase the pullout resistance capacity of soil nail.

Moreover, large diameter of disc will tend to provide large bearing area which should increase the pullout resistance. The effective bearing area of circular disc depends on nail shaft diameter. Similarly, the contribution of shaft friction is affected by circular disc spacing. In order to understand the effect of these variations, several combinations among different parameters have been analysed. The summary of these combinations is given in Fig. 2 and Table 1.

3. 3D finite element model for pullout analysis

The pullout of soil nail with circular discs is carried out by a finite element code Abaqus in 3D space. Abaqus/Explicit provides a sub-routine best suited for analysis of nonlinear behaviour associated with contact between soil nail and surrounding soil continuum (Dassault Systèmes, 2013). The 3D modelling ensures a better understanding of stress conditions around the soil nail during pullout as compared to two-dimensional (2D) modelling where equivalent stiffness method of smearing is used to simulate soil-nail interaction. The 2D analysis underestimates peak pullout force and gives incorrect nail displacement (Kao, 2004). This explains the deficiency of 2D condition in accurately simulating the nonlinear behaviour of soil nail pullout problem which is highly dependent on stresses in soil-nail interface. However, to minimise computational time, researchers in the past have assumed stresses

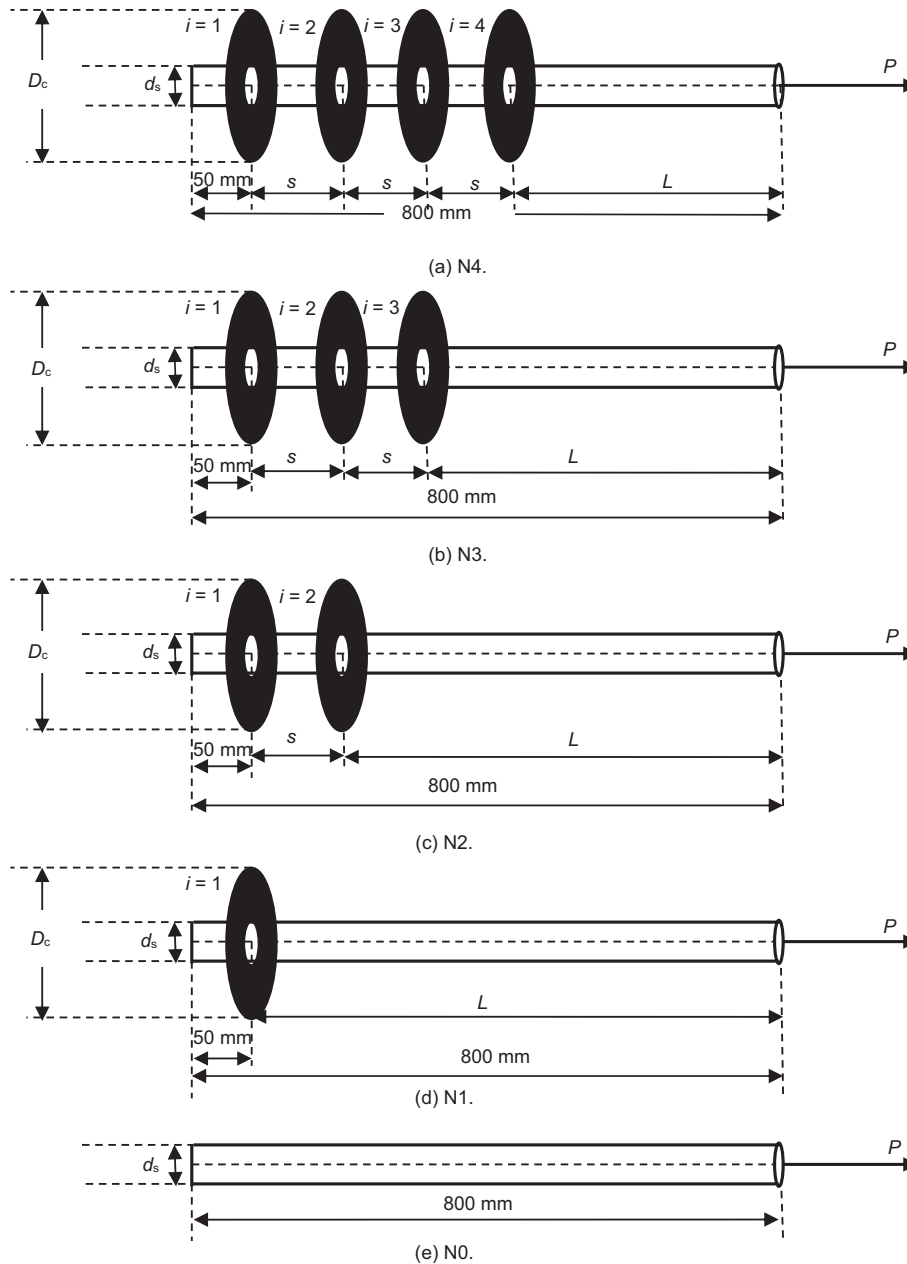


Fig. 2. Different configurations of soil nails with and without circular discs. Notations N4–N0 mean that the number of circular discs along the nail shaft ranges from 4 to 0.

around soil nail as constant, thereby treating it as an axisymmetric problem (Morris, 1999; Kao, 2004; Lum, 2007; Tokhi et al., 2016). To ensure proper nonlinear stress generation around soil–nail interface, 3D numerical modelling thus becomes essential.

3.1. Constitutive model for soil and nail with circular discs

The soil continuum is simulated by using hexahedra (bricks) continuum isoparametric elements of C3 element class in three dimensions. Continuum hexahedra can either be 8-node or 20-node elements. An 8-node linear brick element with reduced integration (C3D8R) is used to model the soil domain. Reducing integration reduces the number of constraints introduced by an element due to internal constraints. According to Dasari and Soga (2000) for problems involving contact and large distortion, the finite element mesh is also highly distorted. Hence use of the first-order elements with reduced integration is recommended. Soil is

modelled as deformable solid with stress–strain behaviour being governed by the modified Drucker–Prager Cap model. The modified Drucker–Prager Cap model is mainly used for pressure-dependent yield materials. The yield surface of Drucker–Prager plasticity model is defined by a shear failure surface for perfectly plastic yield without hardening and a ‘cap’ for plastic compaction and soil softening due to inelastic volume increase (dilatancy). The associated flow is related to ‘cap’ region while shear failure region obeys non-associated flow rule. The non-associated flow rule is commonly adopted when the dilatancy effect is of importance (Seo et al., 2012). The Drucker–Prager failure surface is given by

$$F_s = t - p \tan \beta - d = 0 \tag{4}$$

where β is the angle of friction of material, d is the cohesion, p is the equivalent pressure stress, and t is the deviatoric stress at failure. The Drucker–Prager model in Abaqus is expressed in terms of stress invariants as

Table 1
Different combinations of parameters used in analysis.

Notation	N	d_s (mm)	D_c/d_s	s/D_c	L (mm)	L/D_c	
N4	4	15	4	1	570	9.5	
				1.5	480	8	
				2	390	6.5	
				2.5	300	5	
				3	210	3.5	
				3.5	120	2	
				4	30	0.5	
				3	1	615	13.67
					1.5	547.5	12.16
					2	480	10.67
					2.5	412.5	9.16
					3	345	7.67
					3.5	277.5	6.16
					4	210	4.67
					1	660	22
				2	1.5	615	20.5
					2	570	19
					2.5	525	17.5
					3	480	16
					3.5	435	14.5
4	390	13					
N3	3	15	4		1	630	10.5
					1.5	570	9.5
				2	510	8.5	
				2.5	450	7.5	
				3	390	6.5	
				3.5	330	5.5	
				4	270	4.5	
				3	1	660	14.67
					1.5	615	13.67
					2	570	12.67
					2.5	525	11.67
					3	480	10.67
3.5	435	9.67					
2	4	390	8.67				
	1	690	23				
	1.5	660	22				
	2	630	21				
	2.5	600	20				
	3	570	19				
	3.5	540	18				
	4	510	17				
N2	2	15	4	1	690	11.5	
				1.5	660	11	
				2	630	10.5	
				2.5	600	10	
				3	570	9.5	
				3.5	540	9	
				4	510	8.5	
				3	1	705	15.67
					1.5	682.5	15.16
					2	660	14.67
					2.5	637.5	14.16
					3	615	13.67
					3.5	592.5	13.16
				2	4	570	12.67
					1	720	24
					1.5	705	23.5
					2	690	23
					2.5	675	22.5
3	660	22					
3.5	645	21.5					
4	630	21					
N1	1	15	4	750	12.5		
			3	750	16.67		
			2	750	25		
N0	0	15	1				

$$p = -\frac{1}{3}\text{trace}(\sigma) \quad (5)$$

$$q = \sqrt{\frac{3}{2}\mathbf{S}:\mathbf{S}} \quad (6)$$

$$r = \left(\frac{9}{2}\mathbf{S}:\mathbf{S}\mathbf{S}\right)^{1/3} \quad (7)$$

$$t = \frac{1}{2}q \left[1 + \frac{1}{K} - \left(1 - \frac{1}{K}\right) \left(\frac{r}{q}\right)^3 \right] \quad (8)$$

where q is the Mises equivalent stress, r is the third stress invariant, $\text{trace}(\sigma)$ is the summation of three normal stress components of any stress tensor, σ is the stress tensor, \mathbf{S} is the deviatoric stress, and K is the material parameter that controls the dependence of the yield surface on the value of the intermediate principal stress.

Parameter K in Eq. (8) helps to control the effect of intermediate stress on yield surface. It can be stated that the minimal soil disturbance will take place during the installation process of soil nail with circular discs owing to small thickness of circular plates. However, the modelling in the present work has been carried out from the time when the soil nail has been placed in the soil mass and the surrounding soil has reestablished its contact with the soil nail. In that scenario, the constitutive model for soil-nail interface zone simulation will be similar to that for surrounding soil domain. Hence similar constitutive model is used to simulate the condition. Moreover, since creep is a function of state of packing of sand and is higher for loose sand (Leung et al., 1997), the surrounding soil for the present study consists of drained sandy soil with a high angle of friction of 36.5° rendering it as dense, hence consolidation and creep settlement of surrounding soil are expected to occur within small time interval from the time of installation of nail. This small time interval for consolidation and creep ensures that perfect contact between nail and surrounding soil occurs soon after installation. This signifies that soil properties at and around the soil-nail interface can be treated as similar.

Soil nails are modelled as deformable solid sections consisting of two parts, i.e. shaft and circular disc. The shaft and circular disc simulations respectively consist of 1200 and 216 linear hexahedral elements of type similar to soil continuum defined as C3D8R of first-order. The discs and nail shaft interaction is defined by a surface to surface 'tie' constraint, which permits the same degree of freedom as that of nail shaft. The simulated nail with circular disc is accommodated in a sandy soil domain by assigning a 'penalty-type' contact between surrounding soil and simulated nail. The parameters used for modelling soil domain (Dasari and Soga, 2000) and nail with circular disc are summed up in Table 2.

3.2. Geometry, boundary conditions and pullout modelling

The geometry of pullout box is adopted from laboratory pullout test conducted on screw nail by Tokhi et al. (2016). The box has a length of 1500 mm with 1000 mm in height and 1000 mm in width. The nail with circular discs is placed at a depth (H) of 500 mm from the top surface of model box. The total length of nail used for analysis is 800 mm. The length and location of nail have been selected such that the difference in pullout is less than 5% due to rigid outer boundaries. An optimal radial distance of 25 times the radius of inclusion is found to satisfy this condition (Lum, 2007), which is well within the permitted outer boundary variation for pullout in finite element analysis of 20–50 times the radius of inclusion. The radius of nail used in present analysis is 7.5 mm, which calculates the minimum distance of outer boundary as 187.5 mm. However, the outer boundaries for present model lie well beyond the minimum distance. To simulate the actual boundary conditions, the degree of freedom of all the sides of modelled pullout box has been restricted as $X = 0$, $Y = 0$ and $Z = 0$ at the beginning of analysis. For application of overburden pressure of 20 kPa, top surface of

Table 2
Modelling parameters for soil domain and nail with circular discs.

Medium	Type	Model	Density (kg/m ³)	Elastic modulus, E (MPa)	Poisson's ratio, ν	Cohesion, d (kPa)	Angle of friction, β (°)	Dilation angle, ψ (°)	Flow stress ratio, K^a	Friction coefficient ^b
Soil	Solid, deformable (sand)	Drucker–Prager Cap model	1650	50	0.3	0	36.5	6.5	0.778	0.21
Nail shaft and circular discs	Solid, deformable	Drucker–Prager Cap model	7850	2×10^5	0.3	–	–	–	–	0.21

^a Ratio of flow stress in triaxial tension to that in triaxial compression ($0.778 \leq K \leq 1$) (Dassault Systèmes, 2013).

^b Value of penalty-type friction coefficient adopted from Tokhi et al. (2016).

pullout box is allowed to displace in the vertical downward direction (Y-axis) with all other degrees of freedom being restricted. The pullout of soil nail is carried out in a load-control manner by applying a load of 30 kN at nail head. For this stage of analysis, a small circular opening near the nail head is set free in Z-direction. To ensure quality of meshing, partitioning and finer meshing around shaft and circular disc are carried out. The overburden pressure and pullout load are applied in a series of steps. An initial step is set up to establish equilibrium stress conditions and contact surfaces between soil domain and inclusion. The complete analytical pullout model is shown in Fig. 3.

However, installation mechanism of this type of soil nail has not been modelled in the present analysis. A soil nail with circular disc holds an added advantage over conventional nails by the virtue of its ease of installation. The installation of soil nails mounted with parallel discs in longitudinal direction can be achieved by either embedding the nails during staged construction or by pushing and rotation technique. Moreover, due to small thickness of circular discs, minimal soil disturbance will occur. Also, since the surrounding soil is sand, these soil disturbances will not alter the properties of soil significantly. These soil nails do not require a grout surface and consequently no drill hole is required. To install such nails, torque is provided at the nail head which drives the nail to desired location. This installation technique is believed to produce slight disturbances to the surrounding soil and produce no spoils (Tokhi et al., 2016). Based on the above observation, it is assumed that soil properties during nail installation are not altered significantly and hence installation process modelling prior to pullout has not been included in the present analysis.

4. Results from finite element analysis

A total of 67 simulations has been performed to obtain the pullout load with nail displacement, stresses around the nail during pullout, developed rupture surface in soil and nail, variation in normalised pullout capacity with parametric variation by 3D finite element analysis using Abaqus/Explicit for pullout capacity of a modified soil nail with circular disc along the shaft placed in sandy soil.

4.1. Pullout load

The pullout loads with displacement of soil nail for different circular disc diameters of 30 mm, 45 mm and 60 mm and different numbers of circular discs varying from $N = 1$ to 4 are shown in Fig. 4. It can be observed from Fig. 4a that the peak pullout load is achieved by N4 nail with the maximum load capacity of 20.34 kN at nail displacement of 27.12 mm. The peak pullout load for N3 nail is 18.1 kN and that for N2 nail is 17.41 kN at displacements of 25.4 mm and 24.96 mm, respectively. However, a maximum of 16.51 kN pullout load is obtained for N1 nail with 24.68 mm nail displacement. For N0 nail, the pullout load reaches a value of 11.77 kN with nail displacement of 21.88 mm. Similarly, from Fig. 4b, it can be observed that pullout loads of 19.99 kN, 17.79 kN, 16.8 kN and

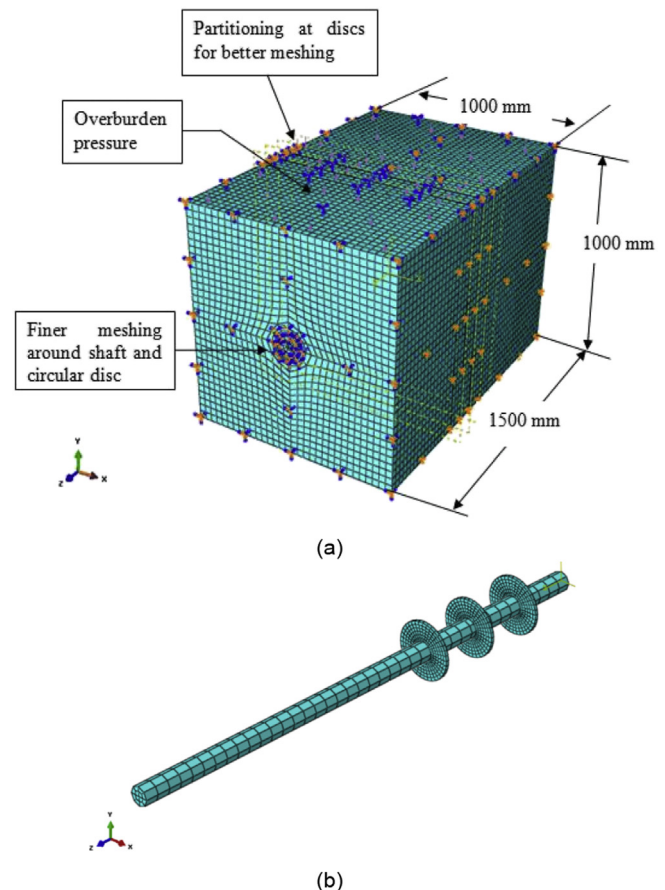


Fig. 3. Dimensions, boundary conditions and finite element meshing for (a) modelled pullout box and (b) modelled soil nail shaft with circular discs.

14.93 kN are obtained for N4, N3, N2 and N1 nails, respectively. The corresponding nail displacements are 26.58 mm, 25.29 mm, 24.84 mm and 24.2 mm, respectively. As the disc diameter decreases from 60 mm to 30 mm, a significant fall in pullout load is also observed. Nail N4 depicts a peak pullout load of 15.04 kN with 25.12 mm displacement, and nail N3 shows a displacement of 25.18 mm and peak load of 15.48 kN. Pullout load of 14.17 kN for N2 nail and 13.35 kN for N1 nail can be observed from Fig. 4c. Nails N2 and N1 attain pullout load at nail displacement of 24.72 mm and 23.73 mm, respectively.

It is a common observation from Fig. 4 that as the number of circular discs increases, it leads to an increase in pullout load. Also, as the diameter of circular disc increases, the pullout load is found to increase. The reason for this variation in pullout capacity can be given on the basis of Eq. (3). It can be seen from Eq. (3) that as the number of discs increases, contribution of circular discs to pullout resistance increases.

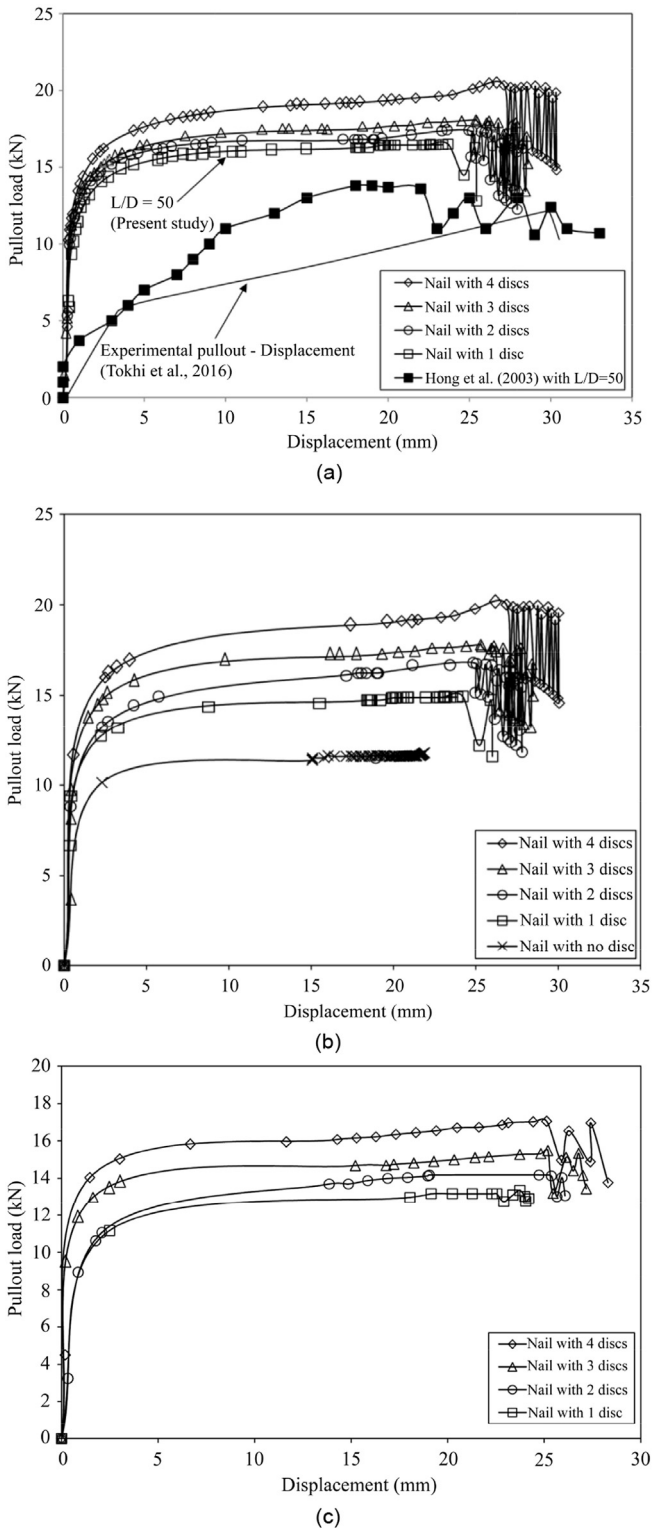


Fig. 4. Pullout load variations with nail displacement for $D_c/d_s =$ (a) 4, (b) 3 and (c) 2.

The physics of increase in pullout resistance with increase in number of discs can be attributed to the densification of soil sandwiched between circular plates during pullout. As a nail with single circular disc moves out under pullout force, local soil influence around circular plate is found. With increase in the number of circular plates, the local soil influence is found to change and soil is influenced to a much greater depth from nail shaft. The soil

sandwiched between two circular plates is compacted due to nail pullout and creates a cylindrical soil mass. This cylindrical soil mass behaves as a composite part of nail. The nail with circular discs now appears as a nail with an enlarged diameter equal to that of circular discs.

This leads to a shift in failure interface from soil-nail for single disc nail to compacted soil-surrounding soil interface for multiple circular discs. For nail with smaller number of discs, shaft friction and plate bearing contribute to pullout resistance, whereas with increase in the number of circular discs, shaft friction effect diminishes and pullout is predominantly governed by bearing from the enlarged diameter due to dense cylindrical soil mass formed between circular discs, as shown in Fig. 5.

As a circular disc is introduced along the nail shaft, it displaces the soil adjacent to it. With increase in the number of circular discs, more soil displacement takes place. This leads to densification of soil lying in a zone sandwiched between two circular discs. The degree of densification of displaced soil will depend upon the spacing of circular discs. Moreover, nail without circular disc (N0) utilises only its shaft friction to resist the pullout force, but with circular discs, an additional bearing component acts along with shaft friction to restrain pullout from soil. Similarly, as the circular disc diameter is increased, the bearing area of disc increases. This increase in bearing area helps nail accommodate large quantity of soil in between circular discs. If the spacing between the discs is small, this compacted soil between two discs will act as a part of nail and move together as one composite unit. Due to this, the shear stresses mobilised at the nail shaft–soil interface are pushed deep into the soil. The shear stresses are now acting on the interface of this compacted soil between discs and surrounding weak soil. Also, with increase in disc diameter, the effective perimeter of nail increases, which contributes significantly to increasing the pullout load.

From Fig. 4a, it can also be observed that as the peak pullout load is attained by soil nails, a sharp reduction in pullout capacity is found. As the nail displacement continues to increase, a rise and fall in pullout load is observed for all nails with discs. Hong et al. (2003) concluded from their study on pullout of single and double soil nails that rough nails depict a profound unsmooth (zigzag) phenomenon of load–displacement curve, whereas a smooth curve is obtained for smooth surface nails. A similar observation has also been reported by Raju (1996). As observed from Fig. 4b, the zigzag profile of load–displacement curve changes to smooth as the number of discs along nail shaft decreases from 4 to 1. A relatively smoother load–displacement curve is obtained for nail without any disc. Another important observation in Fig. 4c is that as the diameter of circular disc decreases and approaches shaft diameter, zigzag pattern of load–displacement curve becomes flatter with small difference between the maximum and minimum pullout

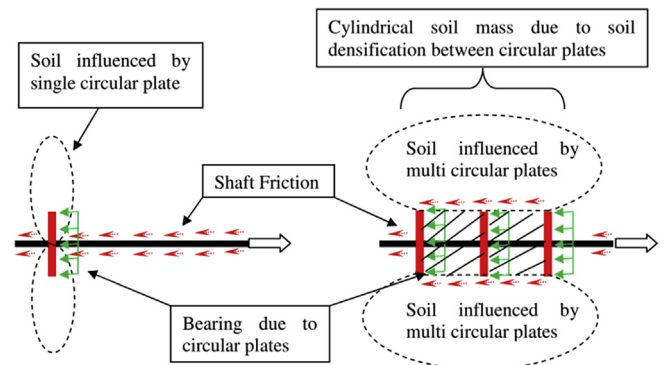


Fig. 5. Pullout resistance with increase in number of discs.

magnitudes. The load–displacement curve for nail N1 with $D_c/d_s = 2$ is comparable to the smooth curve obtained for N0 nail in Fig. 4b. Tokhi et al. (2016) reported a similar curve from laboratory pullout test on screw nails (Fig. 4a), where helical plates of varying diameter for pullout testing in laboratory were used. However, Tokhi et al. (2016) simplified the finite element analysis in terms of meshing problems and analysis time by using circular plates of varying diameter along shaft for simulation of screw nails in Abaqus. By far this is the only available material which can be closely related to the present soil nail with circular discs for validation. However, the nail used by Tokhi et al. (2016) differs geometrically with the soil nail mounted with circular discs, but for finite element analysis, screw soil nail was taken as soil nail with ring plates, hence the comparison is conducted. Moreover, Tokhi et al. (2016) carried out a displacement-controlled pullout test with the maximum pullout load achieved at a displacement of 49 mm. Beyond this displacement, a sudden drop in the pullout force was observed. It can thus be believed that if pullout was carried out to a larger displacement, then a zigzag profile could have also been observed. Also, the finite element analysis was conducted by considering failure at a displacement of 20 mm and hence a plot which ended abruptly was observed. In the absence of literature regarding soil nail with circular discs, comparison is carried out with nails that can be approximated with the present soil nail geometry. Moreover, Hong et al. (2003) studied pullout load capacity with surface roughness for different L/D ratios. With insufficient literature available on this context for nail with circular discs, soil nail used in the present analysis is also treated as a rough nail and similar L/D ratio nail has been compared. The results of Hong et al. (2003) are comparable because similar zigzag pattern is observed to increase with increase in roughness of soil nail. An identical pattern is also observed for the present soil nail, because as the number of discs increases, soil nail roughness can be believed to have increased. This can be observed by an increase in the zigzag pattern from soil nail with 1 disc to 4 discs, respectively.

However, it can be approximated that if further nail displacement would have been allowed, load–displacement curve for screw nails would have also depicted a similar unsmooth curve. The unsmooth (zigzag) nature of these curves can account for soil softening around the nail. As the nail is pulled out, soil softens under large strain. The soil around circular discs detaches itself from the soil mass and begins to move with nail disc. This softening of soil decreases the pullout load. As nail movement continues to progress under pullout load, the soil between two discs is also undergoing densification. This densified soil increases the disc bearing and hence the pullout load. Soil behind the last disc on nail shaft remains detached from the surrounding soil till the end of pullout test, hence all load–displacement curves are found to terminate at a low pullout load magnitude. The smooth curve for N0 nail can be related to perfectly elastoplastic behaviour of soil. The reason for curves to smooth out with decrease in D_c/d_s can be explained by location of shear stresses around the nail. A decrease in D_c leads to less soil displacement which moves the soil–nail interface closer to nail shaft from deep within soil mass. Correspondingly, shear stresses are mobilised at this lightly densified inter-disc soil, i.e. soil between two consecutive discs, to nail shaft interface. As D_c/d_s approaches 2, soil nail pullout behaviour is similar to that of smooth nail or a nail with larger diameter. During pullout, an increase in the volume of soil takes place around the soil nail. This soil dilation is restrained by normal stress around soil nail. As the inter-disc soil is compacted, it imparts a higher overburden stress which increases the normal stress around soil nail. On the other hand, soil between small-diameter discs densifies a relatively smaller soil mass and hence only small increase in normal stress is observed. The soil dilation is not significantly restrained by this normal stress and hence soil nail

with smaller disc diameter can be pulled out of soil mass easily as compared to nails with large disc diameters.

It can be seen from Fig. 6 that as the number of discs increases, an increase in shear stress is observed. The increase in shear stress can account for the fact that with increase in number of discs, a relatively larger soil comes into interaction with the nail. The failure occurs at a new interface corresponding to diameter of the disc mounted on nail shaft. The increase in number of discs leads to higher densification of soil mass around it, thereby increasing the interface friction between compacted soil within discs and weaker surrounding soil. However, the maximum shear stress for different numbers of discs occurs at a relatively smaller displacement as compared to the corresponding pullout load. This signifies that within a small displacement of nail, the bearing due to discs begins to contribute to pullout resistance which leads to compaction of soil. As the pullout of nail continues, shear stress remains almost constant due to continuous yielding and recompaction of soil which effectively shows no further increase or decrease in shear stress.

4.2. Development of stresses during pullout

During the pullout of nail, shear stresses are induced in the soil. The shear stress mobilisation governs the pullout capacity of nail. The stress contours obtained from finite element analysis are given in Figs. 7–11. It can be seen from Fig. 7 that stresses are generated all along the nail shaft with high concentration of stress near the nail end. The stress contours for N0 nail signifies that shear stresses are mobilised at some distance away from the soil–nail interface.

However, from Fig. 8, it can be depicted that development of stresses around N2 nail depends upon the spacing between circular discs. As the spacing is increased from $3D_c$ to $4D_c$, stress contours travel all the way along the shaft and stress the soil near the nail head. This signifies the fact that there exists a critical spacing between circular discs after which stresses are transferred up to the nail head or slope face in case of field pullout of nails. This behaviour of soil nails can be compared to vertical pullout of multi-plate soil anchors which are classified as shallow anchors and deep anchors based on the slip failure surface (Raju, 1996). For deep anchors, the failure surface is local around the anchor plates, whereas if the failure surface propagates to the ground surface, the anchors are termed as shallow anchors. A similar local and global failure surface is also obtained for soil nails under pullout and hence can be categorised as deep soil nails ($s/D_c \leq 3$) and shallow soil nails ($s/D_c > 3$). From Fig. 8c, it can be seen that as N2 nail is pulled out, the soil behind the circular discs is highly stressed. The reason for generation of these high stresses can be due to active earth pressure

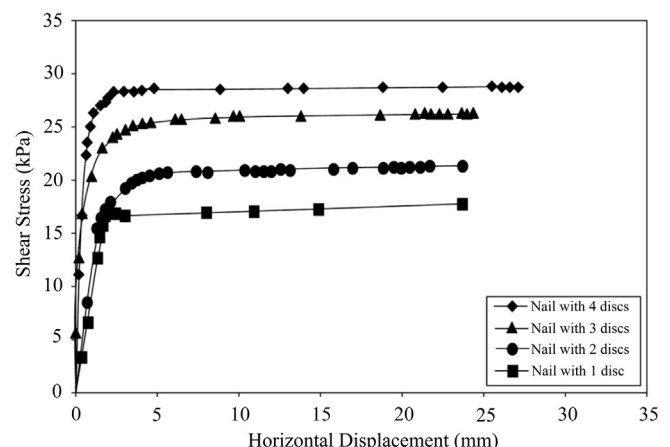


Fig. 6. Shear stress variations with horizontal displacement.

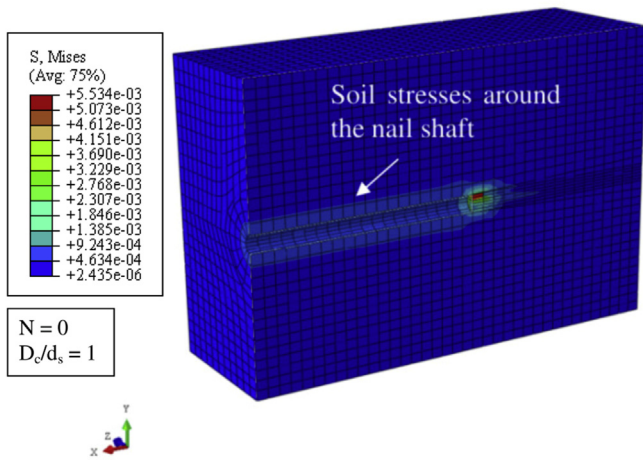


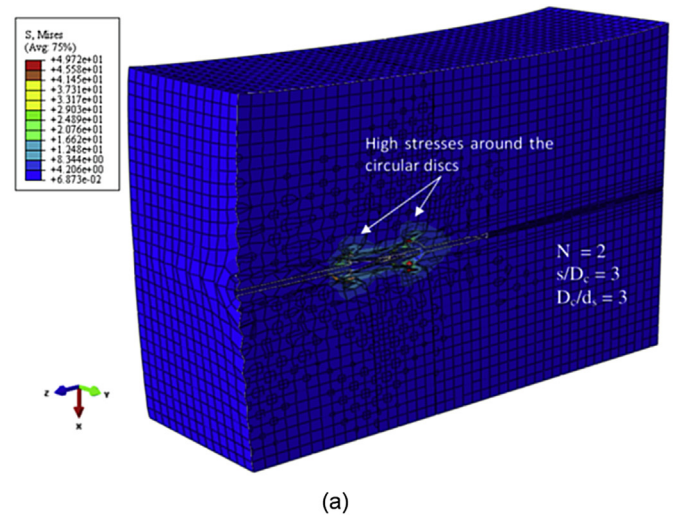
Fig. 7. Stress contours (in kPa) for nail without circular discs ($N = 0$).

condition that develops behind each disc. As the nail moves under pullout force, the soil in front of the discs is in a passive state of earth pressure with active earth pressure acting behind the discs. It can also be seen from Fig. 8c that soil between circular discs becomes densified and moves under pullout force as a part of nail.

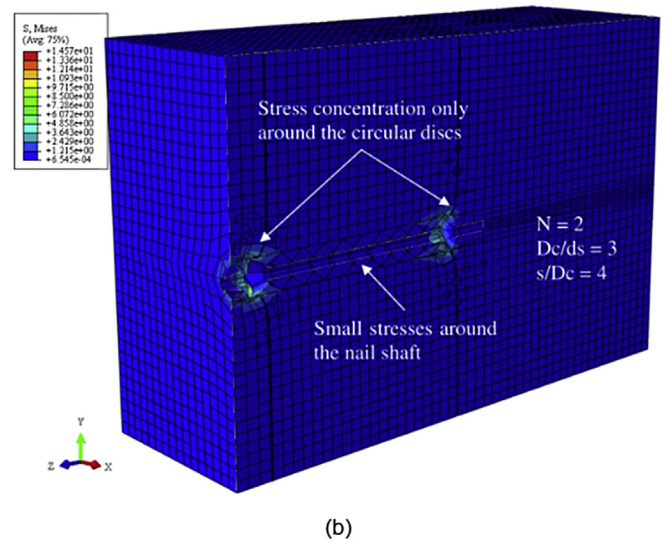
Similar stress contours are observed for N3 nail with $s/D_c = 3$ and 4. The soil between 3 discs is highly stressed with stresses propagating radially towards the nail end. The complete pullout model for N3 nail is shown in Fig. 9a. As observed from cross-section A–A, when the spacing between discs is small, the stress zone is confined around the circular discs. It is obvious to state that failure during pullout occurs at these stressed zones (Fig. 9b). On the other hand, for large spacing between discs, the stress zone extends up to the nail head, thereby a global failure mode can be expected for such soil nails (Fig. 9c). From Fig. 9d, it can be seen through cross-section B–B that soil gets compacted between the discs and forms a cylindrical mass of soil which is highly stressed. During pullout, the interface friction is mobilised at this interface of cylindrical soil mass and surrounding soil rather than nail shaft–soil interface.

For N4 nails, the stress contours follow a similar pattern. The complete pullout model for pullout of soil nail with 4 circular discs is shown in Fig. 10a. The stress contours generated during soil nail pullout are studied by splitting the model through two sections, i.e. A–A and B–B. As shown in Fig. 10b and c, transition in failure mode from local deep failure to global shallow failure is observed with increasing spacing. It can also be observed from the stress contours that high stresses are mainly found between the top two circular discs. As the pullout of nail begins, stresses are mainly concentrated on the nail end. With the nail displacement, the soil mass that detaches itself from the surrounding soil releases its stress and transfers it to the soil mass ahead. In this way, stress progresses in direction of nail displacement. It can also be seen from Fig. 10d that the soil around the circular discs is stressed such that it forms a conical soil mass ahead of each disc. Moreover, the stresses are transmitted radially from discs during soil nail pullout.

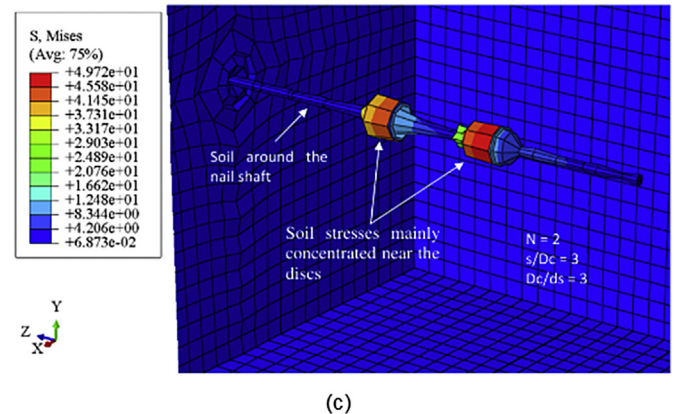
The variation in stresses also occurs if the diameter of circular discs is increased. However, the phenomenon of local and global failure modes still exists. It can be seen from Fig. 11 that by increasing the diameter of circular discs, large soil displacement occurs. This displacement of soil shifts the critical interface deep into the surrounding soil. This reduces the contribution of shaft nail towards pullout resistance but the same is compensated by an increase in the bearing area of circular discs. Hence increasing the diameter of circular disc beyond $D_c/d_s > 3$, pullout capacity of nail should increase or remain constant.



(a)



(b)



(c)

Fig. 8. Stress contours (in kPa) viewed from the side of model tank for N2 nail with (a) $s = 3D_c$ and (b) $s = 4D_c$. (c) 3D stress contours for N2 nail with $s = 3D_c$.

From the stress contour plots, it can be deduced that the rupture surface during pullout of soil nail with circular discs has a defined pattern. The potential rupture surface will consist of a cylindrical soil zone between two discs with a curved conical soil zone in the front of first disc and an extended curved zone around the circular discs. To validate this, the rupture surface as predicted by Tokhi et al. (2016) for pullout of screw nail in laboratory model test can be stated as “Based on the soil deformation patterns, the

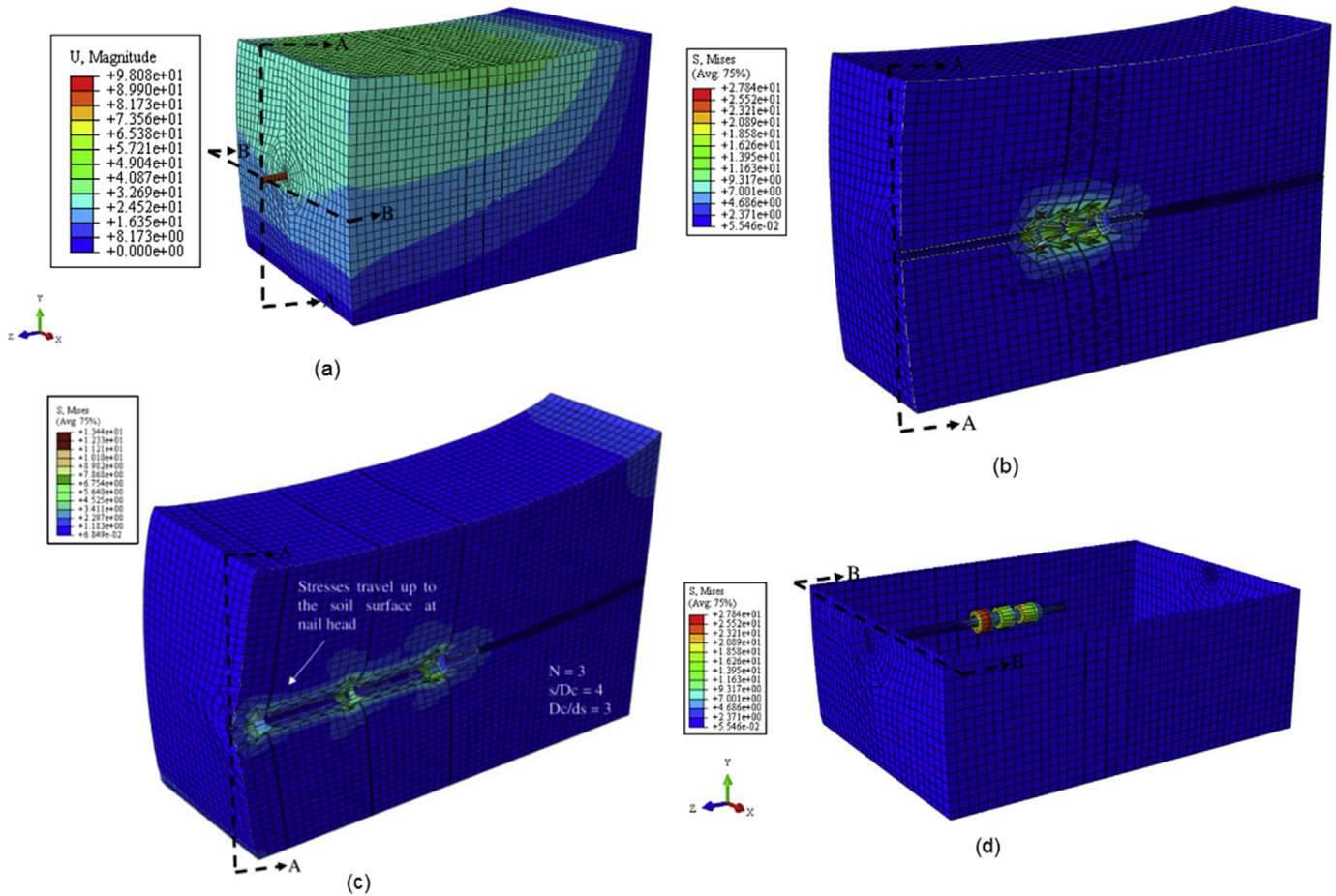


Fig. 9. (a) Complete pullout model for N3 nail. Stress contours (in kPa) viewed from the side of model tank for N3 nail with (b) $s = 3D_c$ and (c) $s = 4D_c$. (d) 3D stress contours for N3 nail with $s = 3D_c$.

area could be separated into three distinct zones: (1) the curved conical zone at the front of rear helix, (2) the extended curved zone around the helix, and (3) extended cylindrical zone approximately between the two helices”.

4.3. Pullout load variation with different combinations of parameters

As shown in Table 1, different combinations of parameters are used to study the pullout load variation. The pullout load for various combinations is converted to a dimensionless factor, normalised pullout load (P/P_0), defined as the ratio of pullout load for the combination under study (P) to pullout load for NO nail (P_0). It can be observed from Fig. 12 that pullout load shows a nonlinear relationship with variation in relative disc spacing ratio (s/D_c). The pullout load increases almost linearly till $s/D_c = 3$, thereby it remains almost constant with increasing s/D_c ratio. This signifies that there lies a critical s/D_c ratio beyond which pullout capacity remains unaffected. This can be well understood from the stress contours shown in Figs. 8–10. For all $s/D_c \leq 3$, soil nails with circular discs act as deep anchors. The failure mode is a local failure of cylindrical soil mass. The increase in pullout capacity up to $s/D_c \leq 3$ can account for compacted soil mass between discs which moves as an integral part of soil nail. The nail now behaves like an enlarged-diameter shaft at the disc level. Moreover, soil densification increases the angle of internal friction of soil between and around the discs. The shear failure occurs at an interface in this densified zone of soil mass just outside the circular disc diameter. The increase in

internal friction also leads to an increase in interface friction, which contributes to increasing the pullout capacity of nail. Beyond $s/D_c > 3$, a transition in failure mode occurs. The deep soil nails shift to behave like shallow soil nails with failure surface reaching the soil around nail head. No compaction of soil occurs between the discs and each disc acts individually in bearing. The contribution of shaft friction to pullout resistance decreases. The pullout capacity of nail is predominantly governed by individual bearing of circular discs. It is also the reason for increase in pullout load beyond $s/D_c > 3$ with increasing N .

The average shear stress of soil-nail interface also follows a similar nonlinear relationship with variation in relative disc spacing ratio (s/D_c) as the pullout load. The average shear stress is found to increase up to a critical relative spacing ratio. The reason for this increase in average shear stress can be the densification of inter-disc soil due to which soil nail now behaves like an enlarged shaft with diameter equal to that of discs. Moreover, soil densification increases the angle of internal friction of soil between and around the discs. The shear failure occurs in this densified zone of soil mass. The increase in internal friction also leads to an increase in interface friction, which contributes to increasing the pullout capacity of nail. Beyond critical relative disc spacing ratio ($s/D_c > 3$), shear stress variation will remain constant due to soil-nail shaft interface which will contribute to shaft friction during pullout resistance. The deep soil nails shift to behave like shallow soil nails with failure surface reaching the soil around nail head. No compaction of soil occurs between the discs and each disc acts individually in bearing. The shear stress contribution will be predominantly governed by shaft friction.

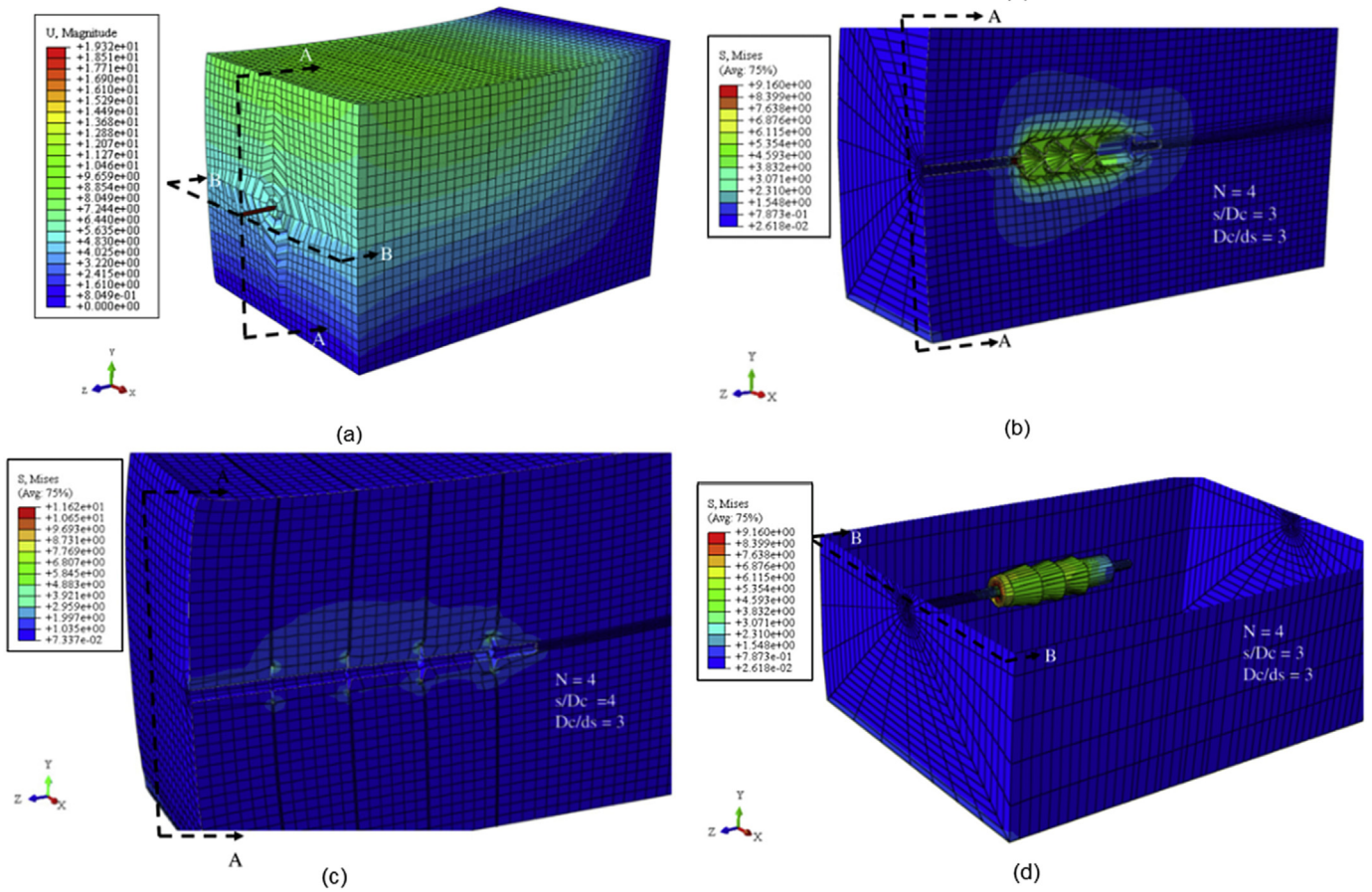


Fig. 10. (a) Complete pullout model for N4 nail. Stress contours (in kPa) viewed from the side of model tank for N4 nail with (b) $s = 3D_c$ and (c) $s = 4D_c$. (d) 3D stress contours for N4 nail with $s = 3D_c$.

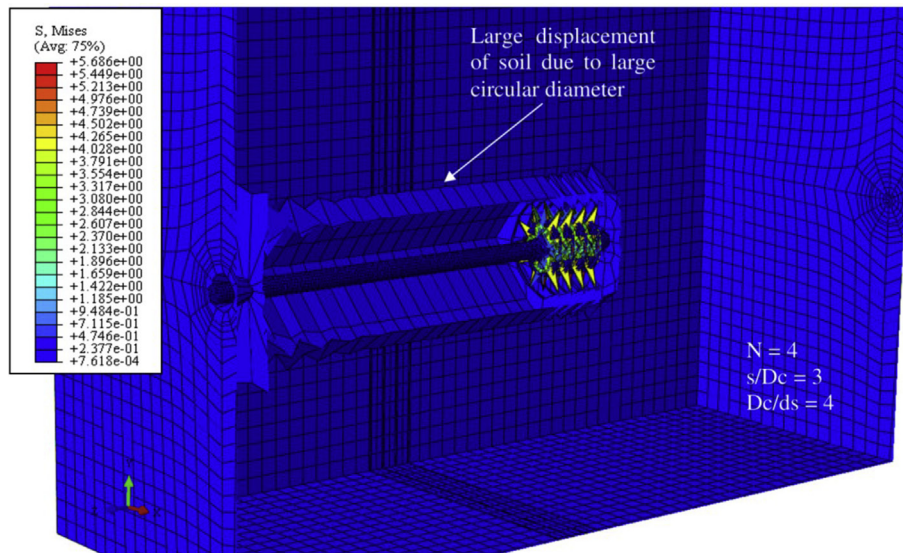


Fig. 11. Stress contours (in kPa) for soil nail with $D_c/d_s = 4$.

Variations of normalised pullout load with anchorage length are shown in Fig. 13. It can be observed that as the anchorage length ratio increases, the normalised pullout load decreases. However, the decrease in normalised pullout load is almost linear up to $L/D_c < 9.16$ for nail with 4 circular discs, $L/D_c < 11.67$ for nail with 3 circular discs, and $L/D_c < 13.67$ for nail with 2 circular

discs. Beyond these L/D_c ratios, a sharp decrease in normalised pullout load is observed. This decrease in pullout load beyond specified L/D_c ratios can be attributed to the contribution of shaft friction to pullout resistance. In order to mobilise the maximum shaft friction, significant length of shaft should extend beyond the passive soil zone. This reduction in shaft friction can only be

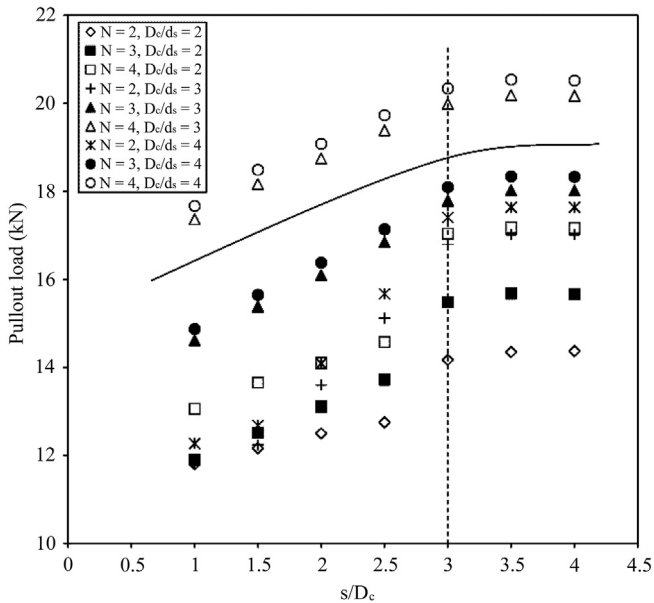


Fig. 12. Variations of pullout load with relative disc spacing ratio.

compensated by increasing the number of circular discs, which increases the bearing capacity of nails against pullout. Hence it can be seen that if the number of circular discs is increased from 2 to 3, a decrease in required anchorage length is found from $13.67D_c$ to $11.67D_c$. Similarly, for increase in number of discs from 3 to 4, required anchorage length decreases from $11.67D_c$ to $9.16D_c$.

The contribution of circular disc bearing with anchorage length variation can also be understood from Fig. 14. A dimensionless bearing capacity factor (N_q) for circular disc bearing has been calculated from Eq. (3). As can be seen from Fig. 14, increase in number of circular discs leads to an increasing bearing of soil nail. Moreover, for soil nails deriving their pullout resistance primarily from bearing, smaller anchorage lengths can be used. It is evident from Fig. 14 that higher anchorage length is observed for soil nails with less number of circular discs. Hence this would lead to a decrease in the bearing component of pullout resistance.

The depth of soil nail below overburden is also found to affect the bearing capacity of soil nails. In the present analysis, embedment ratio is calculated corresponding to change in circular disc diameter with a constant height (H) of overburden above the nail as

500 mm. As shown in Fig. 15, as the embedment ratio (H/D_c) is increased, i.e. diameter of disc is reduced, bearing capacity factor is found to decrease. This signifies that at a constant depth below the overburden, if the diameter of circular discs is reduced, it will lead to decrease in pullout load due to the reduced bearing surface offered by circular discs. However, this reduction in bearing capacity will be smaller for nails having more number of discs. Reducing the circular disc diameter will significantly affect the pullout of nails in order of N_1 nails > N_2 nails > N_3 nails > N_4 nails.

The effect of reduction in circular disc diameter on overall pullout capacity of soil nail can also be understood from Fig. 16. It is evident that as the diameter ratio increases, the normalised pullout load would increase. However, it is interesting to note that this increase in pullout load is significant only up to $D_c/d_s = 3$. Beyond $D_c/d_s > 3$, the increase in pullout load is almost constant. Thus, it can be stated that after a critical diameter ratio of 3, variation in D_c/d_s does not affect the nail pullout load significantly. This can be validated by screw nail design manual (Hubbell Power Systems, Inc., 2015) which states that the diameter of helical plates in a screw soil nail should be equal to a minimum of three times the diameter of shaft. The reason for this variation can be summed up to large soil displacement due to large circular disc diameter. As shown in Fig. 11, soil nail with large-diameter circular discs displaces the soil to a great extent such that no shaft resistance can be utilised by soil nails. The nail shaft moves easily under the pullout force through the dilated soil mass without offering significant

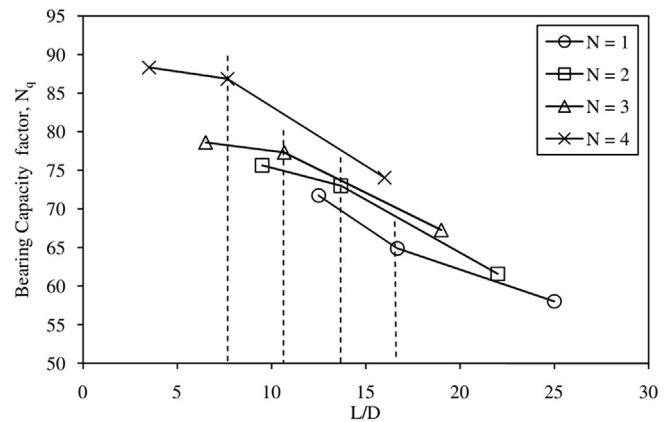


Fig. 14. Variations of bearing capacity factor with anchorage length ratio.

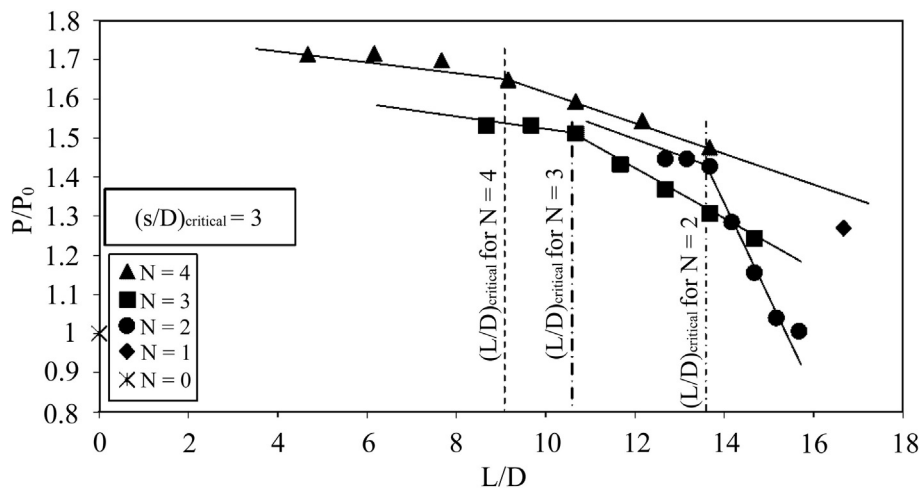


Fig. 13. Variations of normalised pullout load with anchorage length ratio.

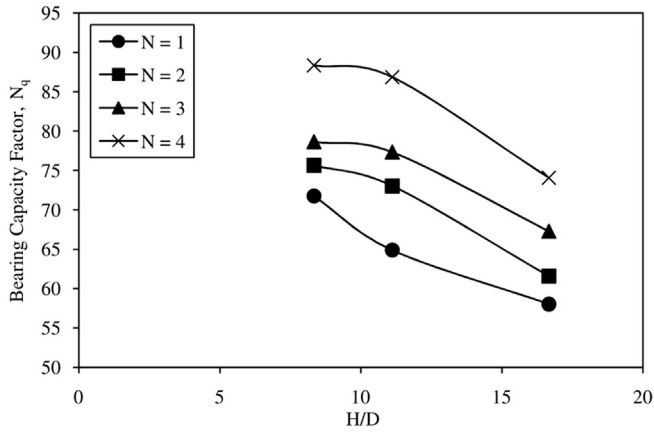


Fig. 15. Variations of bearing capacity factor with embedment depth ratio.

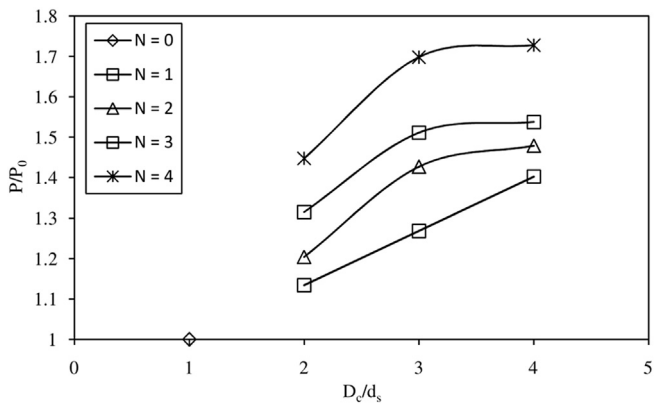


Fig. 16. Variations of normalised pullout load with relative diameter ratio.

resistance. The shear stresses acting on the soil-nail interface are shifted away from nail shaft into a zone marked by restrained dilatancy. This zone where overburden along with normal stress restrains the soil dilation behaviour forms the new interface for

shear stress mobilisation and is dependent on circular disc diameter.

The shear stress at soil-nail interface is mobilised with displacement of nail. However, nail displacement depends upon the anchorage nail length available for pullout. It can be seen from Fig. 17 that as the displacement ratio defined by displacement of nail to anchorage nail length ratio increases, normalised pullout load is found to increase. This increase in pullout load with nail displacement follows a nonlinear path. After a certain nail displacement, the effect on pullout load is constant. Fig. 17 clearly depicts the fact that displacement ratio brings about a steep increase in normalised pullout load initially, but this effect disappears gradually as displacement ratio continues to increase. The increase in the normalised pullout load initially corresponds to the fact that as displacement increases, the entire embedded length develops shaft friction and the disc acts in bearing. However, as the pullout of soil nail continues, the embedded shaft length contributing to shaft friction decreases. The amount of soil in front of the top disc is also decreasing which brings reduction in the bearing capacity of discs. Due to this relative reduction in shaft friction and bearing, the pullout resistance decreases and thus a flatter normalised pullout resistance against displacement ratio is observed for high displacement ratio values. Moreover, normalised pullout load variation also depends on the number of discs on soil nail along with its displacement. A nail with greater number of discs as compared to nail with less number of discs for the same displacement ratio will depict a higher pullout load, due to the increased bearing offered to soil with increase in number of discs.

5. Conclusions

The 3D finite element analysis has been carried out using Abaqus/Explicit code to study the pullout behaviour of soil nail consisting of circular discs along the shaft. From the analytical results obtained, the following conclusions can be drawn:

- (1) The 3D finite element analysis can accurately predict the nonlinear behaviour of stresses during the pullout of soil nail with circular discs. The results obtained for nail pullout load

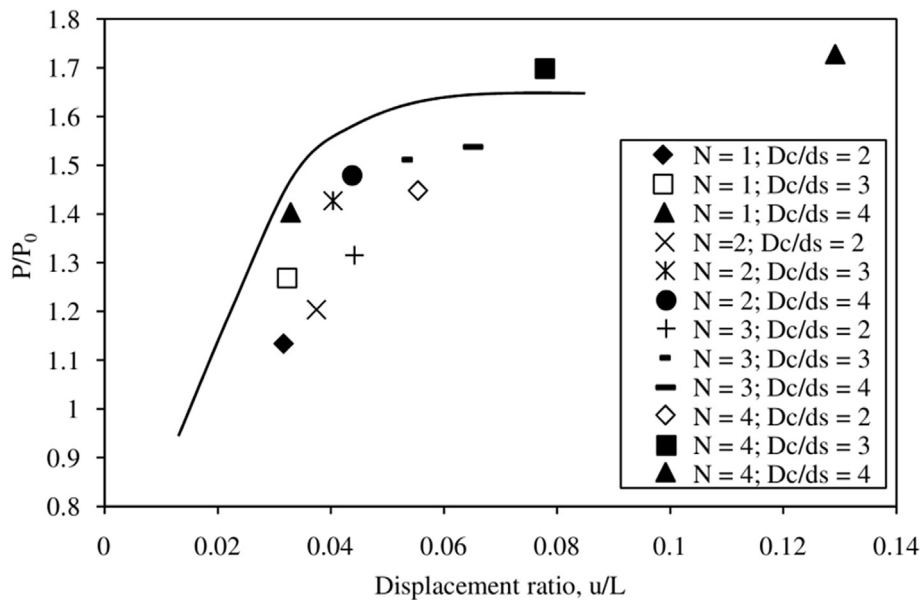


Fig. 17. Variations of normalised pullout load with displacement ratio.

- with nail displacement are in good agreement with experimental and analytical results published in the literature.
- (2) With the introduction of circular discs along nail shaft, pullout load–displacement curves depict an unsmooth pattern due to strain softening in soil as compared to pullout of smooth surface soil nails that follows perfectly elastoplastic soil behaviour.
 - (3) Addition of circular discs increases the pullout capacity of soil nail due to the contribution of circular disc bearing area. It can be concluded that more number of discs yields greater pullout capacity.
 - (4) The stresses around a soil nail with circular discs are different from soil nail without disc. A nail without disc has stresses distributed throughout the nail shaft, whereas with circular discs, location of stresses zone depends upon the disc spacing.
 - (5) There lies a critical relative disc spacing ratio $s/D_c = 3$, which brings transition in the load transfer mechanism of soil nail during pullout. At $s/D_c \leq 3$, pullout is predominantly resisted by a cylindrical soil zone between discs. However, at $s/D_c > 3$, individual bearing capacity of discs governs the soil nail pullout. Furthermore, it can be concluded that failure mode of soil nails during pullout changes from deep local failure around discs to shallow global failure at ground surface, also depending on critical relative disc spacing ratio. Based on the respective modes of failure, soil nails can also be categorised into shallow nails and deep nails similar to multi-plate anchors.
 - (6) The rupture surface during pullout of soil nail with circular discs consists of three zones, i.e. a cylindrical zone between the discs, an extended conical zone in the front of first disc, and curved zone around the discs similar to pullout testing of screw soil nails.
 - (7) The pullout load increases with increase in relative spacing ratio up to $s/D_c = 3$, beyond which it has negligible effect on soil nail pullout load. The normalised pullout load decreases with increase in anchorage length ratio. Nails with greater number of discs require smaller anchorage length. These nails also depict high bearing capacity factor for smaller anchorage length ratios. The bearing capacity factor for nails with more number of circular discs decreases with increase in embedment ratio. However, this decrease is more significant for nails with less number of circular discs. There also exists a critical diameter ratio $D_c/d_s = 3$ to attain a maximum normalised pullout load. The normalised pullout load increases with increase in displacement ratio. However, pullout load becomes constant after a specified nail displacement.
 - (8) It can be concluded that since normal stress significantly affects shaft friction and circular disc bearing, the effect of increasing overburden on soil nails with circular discs can thus be studied in future work.

Conflict of interest

The authors wish to confirm that there are no known conflicts of interest associated with this publication and there has been no significant financial support for this work that could have influenced its outcome.

References

- Akiş E. The effect of group behavior on the pull-out capacity of soil nails in high plastic clay. PhD Thesis. Middle East Technical University; 2009.
- Bridle RJ, Davies MCR. Analysis of soil nailing using tension and shear: experiment observations and assessment. Proceedings of the Institution of Civil Engineers – Geotechnical Engineering 1997;125(3):155–67.

- Dasari GR, Soga K. A guide book for soil models and soil–pipe analysis using Abaqus. Tokyo, Japan: Tokyo Gas; 2000.
- Federal Highway Administration (FHWA). Geotechnical engineering circular No. 7–soil nail walls. Publication No. FHWA0-IF-03–017. Washington, D.C., USA: FHWA; 2003.
- Geotechnical Engineering Office (GEO). Geoguide 7–guide to soil nail design and construction. GEO report No. 197. Hong Kong, China: GEO, Civil Engineering and Development Department, The Government of the Hong Kong Special Administrative Region; 2008.
- Heymann G, Rohde AW, Schwartz K, Friedlaender E. Soil nail pullout resistance in residual soils. In: Proceedings of the International Symposium on Earth Reinforcement Practice; 1992. p. 487–92.
- The Hong Kong Institution of Engineers (HKIE). Soil nails in loose fill slopes. A preliminary study – final report. Hong Kong, China: Geotechnical Division, HKIE; 2003.
- Hong YS, Wu CS, Yang SH. Pullout resistance of single and double nails in a model sandbox. Canadian Geotechnical Journal 2003;40(5):1039–47.
- Hubbell Power Systems, Inc. Soil screw design manual. Centralia, USA: Hubbell Power Systems, Inc.; 2015.
- Juran I. Reinforced soil systems – application in retaining structures. Geotechnical Engineering 1985;16(1):39–82.
- Kao XL. Numerical modelling of anchor–soil interaction. PhD Thesis. Singapore: National University of Singapore; 2004.
- Leung CF, Lee FH, Yet NS. The role of particle breakage in pile creep in sand. Canadian Geotechnical Journal 1997;33(6):888–98.
- Lum CW. Static pullout behaviour of soil nails in residual soil. PhD Thesis. Singapore: National University of Singapore; 2007.
- Luo SQ, Tan SA, Yong KY. Pull-out resistance mechanism of a soil nail reinforcement in dilative soils. Soils and Foundations 2000;40(1):47–56.
- Merifield RS. Ultimate uplift capacity of multiplate helical type anchors in clay. Journal of Geotechnical and Geoenvironmental Engineering 2011;137(7):704–16.
- Milligan GW, Tei K. The pull-out resistance of model soil nails. Soils and Foundations 1998;38(2):179–90.
- Morris JD. Physical and numerical modelling of grouted nails in clay. PhD Thesis. Oxford, UK: University of Oxford; 1999.
- Papadopoulou K, Saroglou H, Papadopoulos V. Finite element analyses and experimental investigation of helical micropiles. Geotechnical and Geological Engineering 2014;32(4):949–63.
- Perko HA. Energy method for predicting installation torque of helical foundations and anchors. In: New technological and design developments in deep foundations. American Society of Civil Engineers; 2000. p. 342–52.
- Pradhan B, Tham LG, Yue ZQ, Junaideen SM, Lee CF. Soil–nail pullout interaction in loose fill materials. International Journal of Geomechanics 2006;6(4):238–47.
- Raju GVR. Behaviour of nailed soil retaining structures. PhD Thesis. Singapore: Nanyang Technological University; 1996.
- Rawat S, Gupta AK. Numerical modelling of pullout of helical soil nail. Journal of Rock Mechanics and Geotechnical Engineering 2017;9(4):648–58.
- Schlosser F. Behaviour and design of soil nailing. In: Proceedings of recent developments in ground improvement techniques; 1982. p. 399–413.
- Seo HJ, Jeong KH, Choi H, Lee IM. Pullout resistance increase of soil nailing induced by pressurized grouting. Journal of Geotechnical and Geoenvironmental Engineering 2012;138(5):604–13.
- Su LJ, Yin JH, Zhou WH. Influences of overburden pressure and soil dilation on soil nail pull-out resistance. Computers and Geotechnics 2010;37(4):555–64.
- Dassault Systèmes. Abaqus v6.13 User's manual. Dassault Systèmes; 2013.
- Tokhi H, Ren G, Li J. Laboratory study of a new screw nail and its interaction in sand. Computers and Geotechnics 2016;78:144–54.
- Yin J, Su L. An innovative laboratory box for testing nail pull-out resistance in soil. Geotechnical Testing Journal 2006;29(6):451–61.
- Zhou W. Experimental and theoretical study on pullout resistance of grouted soil nails. PhD Thesis. Hong Kong, China: Hong Kong Polytechnic University; 2008.
- Zhou YD, Cheuk CY, Tham LG. Numerical modelling of soil nails in loose fill slope under surcharge loading. Computers and Geotechnics 2009;36(5):837–50.
- Zhou WH, Yin JH, Hong CY. Finite element modelling of pullout testing on a soil nail in a pullout box under different overburden and grouting pressures. Canadian Geotechnical Journal 2011;48(4):557–67.



Professor Ashok Kumar Gupta is Head of Department of Civil Engineering, Jaypee University of Information Technology (JUIT), Waknaghat, Solan, Himachal Pradesh, India. He obtained his Bachelor of Engineering degree from University of Roorkee (now IIT Roorkee), MEng degree from University of Roorkee in 1986, and PhD of Civil Engineering from IIT Delhi in 2000. His research interests cover testing and modelling of geotechnical materials, finite element modelling and its applications to geotechnical engineering, continuum damage mechanics and its application to rockfill materials modelling, and engineering rock mechanics. He is Founder Chairman of Indian Geotechnical Society (IGS) Shimla Chapter.